Cell PRESS
Chemistry & Biology
Article

PI3K-δ and PI3K-γ Inhibition by IPI-145 Abrogates Immune Responses and Suppresses Activity in Autoimmune and Inflammatory Disease Models

David G. Winkler,[1] Kerrie L. Faia,[1] Jonathan P. DiNitto,[1] Janid A. Ali,[1] Kerry F. White,[1] Erin E. Brophy,[1] Melissa M. Pink,[1] Jennifer L. Proctor,[1] Jennifer Lussier,[1] Christian M. Martin,[1] Jennifer G. Hoyt,[1] Bonnie Tillotson,[1] Erin L. Murphy,[1] Alice R. Lim,[1] Brian D. Thomas,[1] John R. MacDougall,[1] Pingda Ren,[2] Yi Liu,[2] Lian-Sheng Li,[2] Katti A. Jessen,[2] Christian C. Fritz,[1] Joi L. Dunbar,[1] James R. Porter,[1] Christian Rommel,[2,3] Vito J. Palombella,[1] Paul S. Changelian,[1,*] and Jeffery L. Kutok[1,*]
[1]Infinity Pharmaceuticals, Inc., Cambridge, MA 02139, USA
[2]Intellikine, Inc., La Jolla, CA 92037, USA
[3]Present address: Amgen Inc., Thousand Oaks, CA 91320, USA
*Correspondence: paul.changelian@infi.com (P.S.C.), jeff.kutok@infi.com (J.L.K.)
http://dx.doi.org/10.1016/j.chembiol.2013.09.017

SUMMARY

Phosphoinositide-3 kinase (PI3K)-δ and PI3K-γ are preferentially expressed in immune cells, and inhibitors targeting these isoforms are hypothesized to have anti-inflammatory activity by affecting the adaptive and innate immune response. We report on a potent oral PI3K-δ and PI3K-γ inhibitor (IPI-145) and characterize this compound in biochemical, cellular, and in vivo assays. These studies demonstrate that IPI-145 exerts profound effects on adaptive and innate immunity by inhibiting B and T cell proliferation, blocking neutrophil migration, and inhibiting basophil activation. We explored the therapeutic value of combined PI3K-δ and PI3K-γ blockade, and IPI-145 showed potent activity in collagen-induced arthritis, ovalbumin-induced asthma, and systemic lupus erythematosus rodent models. These findings support the hypothesis that inhibition of immune function can be achieved through PI3K-δ and PI3K-γ blockade, potentially leading to significant therapeutic effects in multiple inflammatory, autoimmune, and hematologic diseases.

INTRODUCTION

Phosphoinositide-3 kinases (PI3Ks) are key cellular signaling proteins that act as a central node for relaying signals from cell-surface receptors to downstream mediators (Bi et al., 1999; Clayton et al., 2002; Cushing et al., 2012; Hirsch et al., 2000; Kulkarni et al., 2011; Puri and Gold, 2012). PI3Ks are lipid kinases that phosphorylate the 3-position of phosphatidylinositol lipids to create phosphatidylinositol-3,4,5-trisphosphate (PIP_3). Membrane-anchored PIP_3 acts as a docking site for multiple signaling proteins, leading to the activation of downstream effectors such as AKT and BTK. The class IA PI3Ks are heterodimers composed of a regulatory subunit (p85) and three different catalytic subunits (p110-α, p110-β, and p110-δ) encoded by three homologous genes (*PIK3CA*, *PIK3CB*, and *PIK3CD*). In contrast, class IB contains a single member that utilizes unique related regulatory subunits (p101 and p84) with the catalytic subunit p110-γ encoded by the gene *PIK3CG*. Recent work has revealed surprisingly different tissue expression levels and functions for individual isoforms. PI3K-α is ubiquitously expressed and genetic knockout of this isoform in mice is embryonically lethal (Bi et al., 1999). PI3K-β knockouts exhibit a variable phenotype ranging from embryonic lethality in some strains to defects in platelet aggregation and neutrophil function in others (Kulkarni et al., 2011). In contrast, ablation of PI3K-δ and PI3K-γ generates viable, fertile mice that reveal defects in their immune system (Clayton et al., 2002; Cushing et al., 2012; Hirsch et al., 2000; Jou et al., 2002; Kulkarni et al., 2011; Puri and Gold, 2012; Sasaki et al., 2000).

The important role of PI3K-δ and PI3K-γ in adaptive and innate immunity has been explored in murine knockout and kinase-inactive knockin mutant animals (Al-Alwan et al., 2007; Bilancio et al., 2006; Clayton et al., 2002; Condliffe et al., 2005; Cushing et al., 2012; Dil and Marshall, 2009; Durand et al., 2009; Garçon et al., 2008; Haylock-Jacobs et al., 2011; Hirsch et al., 2000; Jou et al., 2002; Liu et al., 2007; Okkenhaug et al., 2002, 2006; Pinho et al., 2007; Puri and Gold, 2012; Sasaki et al., 2000; Soond et al., 2010). PI3K-δ mediates signaling through receptor tyrosine kinases, cytokine receptors, integrins, B and T cell receptors, and Fc epsilon receptor 1 (FcεR1). Examinations of PI3K-δ-deficient or kinase-impaired mice have linked PI3K-δ to the activation and proliferation of B and T cells, differentiation of T helper 1 (TH1) and TH17 inflammatory cells, and effective signaling in basophils, mast cells, monocytes, macrophages, and dendritic cells (Al-Alwan et al., 2007; Bilancio et al., 2006; Clayton et al., 2002; Condliffe et al., 2005; Dil and Marshall, 2009; Durand et al., 2009; Garçon et al., 2008; Haylock-Jacobs et al., 2011; Liu et al., 2007; Okkenhaug et al., 2002, 2006; Pinho et al., 2007; Roller et al., 2012; Soond et al., 2010). In contrast, PI3K-γ is linked to chemokine receptor signaling through G protein-coupled receptors (GPCR) and RAS-mediated signaling. Murine PI3K-γ knockout and kinase-dead knockin studies highlighted a vital role for this isoform in T cell development, T leukocyte trafficking, Th1/Th17 responses, T cell receptor-induced

CD4+ T cell activation and proliferation, dendritic cell migration, and neutrophil and monocyte activation and migration (Konrad et al., 2008; Liu et al., 2007; Schmid et al., 2011). This work provides strong evidence that the combined effects of PI3K-δ and PI3K-γ activity are essential for a wide array of adaptive and innate immune functions.

Due to the immune-cell-specific expression and nonoverlapping roles of PI3K-δ and PI3K-γ, loss of activity of both isoforms has broader effects on adaptive and innate immune function than loss of one alone. Mice lacking these isoforms show enhanced resistance to models of inflammatory and autoimmune-mediated diseases. For example, murine knockouts of either PI3K-δ or PI3K-γ alone showed reduced joint injury in a serum-induced arthritis model; however, PI3K-δ,γ double-knockout mice possessed even greater resistance to arthritis induction (Randis et al., 2008). Additionally, the differential effects of PI3K-δ or PI3K-γ inhibition are evident in rodent models of airway inflammation. In these models, mice lacking PI3K-γ exhibit reduced levels of eosinophilic airway inflammation and reduced peribronchial fibrosis (Takeda et al., 2009), whereas animals lacking PI3K-δ display a similar reduction in the levels of eosinophil recruitment and additionally demonstrate a reduced type 2 cytokine response (Nashed et al., 2007).

IPI-145 (also known as INK-1197), a small-molecule inhibitor of PI3K-δ and PI3K-γ, was designed (L.-S.L., K. Chan, K.A.J., L. Darjania, L. Kessler, J. Kucharski, J. Stewart, U. Banerjee, M. Elia, J. Staunton, A. Luzader, M. Zhang, Y. Su, D. Shao, M. Martin, Y.L., G. Birrane, N. Khudaynazar, S. Smith, C.M.M., T.T. Tibbitts, C. Evans, A.C. Castro, C.R., and P.R., unpublished data) to investigate the hypothesis that simultaneous inhibition of these isoforms would demonstrate broad adaptive and innate immune cell inhibitory activity and enhanced efficacy in inflammatory diseases, autoimmune diseases, and hematologic malignancies. A broad array of biochemical and functional cell-based assays demonstrate that IPI-145 is a potent inhibitor of PI3K-δ and PI3K-γ kinase activity. In this work, we explored the therapeutic value of combined PI3K-δ and PI3K-γ blockade with IPI-145 in a rat collagen-induced arthritis (CIA) model, a rat ovalbumin (OVA)-induced asthma model, and a spontaneous murine model of systemic lupus erythematosus. Our findings demonstrate that combined inhibition of adaptive and innate immune function can be achieved through PI3K-δ and PI3K-γ blockade, leading to significant therapeutic effects in multiple inflammatory and autoimmune diseases. Moreover, given the key role of PI3K-δ and PI3K-γ in immune cell function, targeting these isoforms may provide opportunities to develop differentiated therapies for the treatment of hematologic malignancies.

RESULTS

IPI-145 Is a Potent Inhibitor of PI3K-δ and PI3K-γ

The significant, often nonoverlapping roles that the PI3K-δ and PI3K-γ isoforms play in immune cells motivated us to identify small-molecule inhibitors that target both isoforms. An optimization effort resulted in the discovery of a potent oral inhibitor of PI3K-δ and PI3K-γ, the isoquinolinone derivative IPI-145 (Figure 1A). To determine the affinity of IPI-145 for all PI3K isoforms, the individual rate constants (k_{off} and k_{on}) were measured, yielding the K_D for each PI3K isoform (Figure 1B; Figure S1 available online). The K_D values for the class I PI3K isoforms were determined to be 0.023 nM for PI3K-δ, 0.24 nM for PI3K-γ, 1.56 nM for PI3K-β, and 25.9 nM for PI3K-α (Figure 1B). The k_{on} and k_{off} determinations for IPI-145 on PI3K-δ are shown as an example in Figures 1C–1E. The remarkable affinity, and in particular the k_{off}, of IPI-145 for its target predicts a long average target residence time of 45 min per PI3K-δ molecule, which may translate to more durable pharmacodynamic effects. For comparison, the affinity of the PI3K-δ specific inhibitor, GS-1101 (formerly CAL-101) (Lannutti et al., 2011), was also determined for PI3K-δ and PI3K-γ, yielding K_D values of 0.273 nM and 85.7 nM, respectively (Table S1). The structural differences between IPI-145 and GS-1101 have a significant and surprising impact on the binding affinities for PI3K-δ and PI3K-γ. IPI-145 is an ATP-competitive inhibitor; therefore, we determined the relative potencies of IPI-145 for the different PI3K isoforms by using an enzymatic assay to monitor the hydrolysis of ^{32}P ATP at physiological (3 mM) concentrations. This assay yielded IC_{50} values for PI3K-δ and PI3K-γ of 2.5 nM and 27 nM, respectively, and IC_{50} values of 1602 nM and 85 nM for the PI3K-α and PI3K-β isoforms, respectively (Figures 1B and 1F).

To determine kinase selectivity, IPI-145 was screened against a panel of 442 diverse kinases, comprised of 386 nonmutant and 56 mutant kinases, utilizing KINOMEscan technology. IPI-145 selectively bound to PI3K class I isoforms with no significant activity against any other protein or lipid kinases, including class II PI3Ks. Furthermore, IPI-145 was selective against a panel of 50 GPCRs, ion channels, and transporters (Tables S2 and S3).

IPI-145 Is a Potent Inhibitor of PI3K-δ and PI3K-γ Activity in Cellular Assays

Assays designed to allow activity readouts for individual PI3K isoforms were used to assess IPI-145 in a cellular context. To assess PI3K-δ isoform inhibition, the B cell receptor of the human lymphoma cell line RAJI was cross-linked with an anti-immunoglobulin M (anti-IgM) antibody. In this PI3K-δ-specific cellular assay, IPI-145 inhibited pSer473-Akt phosphorylation with an average IC_{50} value of 0.36 nM (Table 1). IPI-145 was ~14 times more potent than the PI3K-δ-specific inhibitor GS-1101 when compared directly (Table S1). Next, the ability of IPI-145 to inhibit PI3K-γ was assessed by measuring AKT phosphorylation in the murine macrophage-like cell line RAW 264.7 after a 3 min stimulation with the complement component fragment C5a, a GPCR agonist (Pinho et al., 2007). IPI-145 inhibited PI3K-γ in C5a-activated RAW cells with an average IC_{50} value of 19.6 nM. Cellular assessment of PI3K-α and PI3K-β inhibition was completed using SKOV-3 (human ovarian adenocarcinoma) and 786-O (human renal cell carcinoma) cell lines, which predominantly express constitutively active PI3K-α or PI3K-β, respectively. In these experiments, IPI-145 generated an average IC_{50} value of 1,410 nM and 26.2 nM for cellular inhibition of PI3K-α and PI3K-β, respectively (Table 1).

IPI-145 Is Active in PI3K-δ- and PI3K-γ-Driven Immune Functional and Whole-Blood Assays

Given the potent cellular activity of IPI-145 against PI3K-δ and PI3K-γ, we next explored isoform-dependent immune cell function. Since PI3K-δ has been described as essential for B cell and T cell proliferation (Okkenhaug et al., 2002, 2006; Pinho et al.,

A

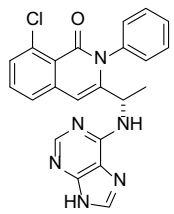

B

IPI-145 binding data	PI3K-α	PI3K-β	PI3K-δ	PI3K-γ
k_{off} (s^{-1})	0.109	0.00426	0.000365	0.000832
k_{on} (10^6 M^{-1} s^{-1})	4.20	2.73	15.6	3.43
t 1/2 (min)	0.10	2.7	31.6	13.8
K_D (nM)	25.9	1.56	0.023	0.24
IC_{50} Enzymatic assay at 3mM ATP (nM)	1602	85	2.5	27

Figure 1. IPI-145 Is a Potent and Selective Inhibitor of PI3K-δ and PI3K-γ

(A) Chemical structure of IPI-145.

(B) Summary of IPI-145 PI3K isoform affinity and binding-rate constants k_{on} and k_{off}. IC_{50} values for IPI-145 against each PI3K isoform were determined at 3 mM ATP by monitoring the amount of radiolabeled ADP and ATP present as a function of IPI-145 concentration (see also Figure S1 and Supplemental Experimental Procedures).

(C) The concentration- and time-dependent decrease of PI3K intrinsic fluorescence upon compound binding was measured with a stopped-flow fluorimeter. Traces were fit to a single exponential function to determine the observed on-rate (k_{obs}).

(D) Plot of k_{obs} versus IPI-145 concentration, with k_{on} determined by the slope of the least-squares linear fit. The linear relationship is indicative of a simple one-step binding mechanism with no induced conformational change following binding.

(E) The off-rate was determined by competing the radiolabeled IPI-145:PI3K-δ complex with excess unlabeled IPI-145. Compound dissociation was measured over time after the addition of excess unlabeled IPI-145.

(F) Isotherms of IPI-145 inhibitory activity in enzymatic assays were determined by monitoring the hydrolysis of 3 mM ^{32}P ATP, with PI3K-α, PI3K-β, PI3K-γ, and PI3K-δ as labeled.

See also Figure S1 and Tables S1–S3.

2007; Soond et al., 2010), we measured the effect of IPI-145 on those activities. Human peripheral blood $CD19^+$ B cells were stimulated with anti-IgM and anti-CD40 antibodies in the presence or absence of IPI-145 for 96 hr. IPI-145 inhibited human B cell proliferation with an average IC_{50} value of 0.5 nM (Table 1; Figure S2A). To test the effect of IPI-145 on T cell proliferation, human peripheral blood $CD3^+$ T cells were stimulated with Concanavalin A (ConA) in the presence or absence of IPI-145 for 72 hr. IPI-145 inhibited the proliferation of stimulated T cells with an average IC_{50} value of 9.5 nM (Table 1; Figure S2B). These data suggest that B and T cell proliferation can be inhibited by IPI-145.

The PI3K pathway plays a critical role in the activation of basophils by relaying signals from cell-surface receptors to downstream mediators (Cushing et al., 2012; Puri and Gold, 2012). Whereas stimulation via the immunoglobulin E (IgE) Fc receptor by the addition of anti-FcεR1 antibody occurs through PI3K-δ, stimulation with formyl-methionyl-leucyl-phenylalanine (*f*MLP) occurs primarily through PI3K-γ. When these two basophil stimuli were used in whole blood, IPI-145 inhibited PI3K-δ-specific degranulation of basophils with an average IC_{50} value of 96.1 nM, and PI3K-γ-specific degranulation with an average IC_{50} value of 1,028 nM (Table 1; Figures S2C and S2D). The finding of higher IC_{50} values in the whole-blood assays compared with the isoform-specific cellular assays (plasma protein-free) is consistent with protein-binding determinations for IPI-145, which indicate it is 86%–96% protein bound in human plasma at these concentrations. At higher concentrations,

Table 1. IPI-145-Mediated Inhibition of PI3K-δ and PI3K-γ Function in Cellular Assays

Cells	Isoform	Stimuli	Conditions	Readout	IC_{50} (nM)
RAJI	PI3K-δ	αIgM	serum free	pS473-Akt	0.36 ± 0.09 (n = 15)
RAW 264.7	PI3K-γ	C5a	serum free	pS473-Akt	19.6 ± 9.0 (n = 30)
786-O	PI3K-β	none	10% FCS	pS473-Akt	26.2 ± 10.2 (n = 6)
SKOV-3	PI3K-α	none	10% FCS	pS473-Akt	1,410 ± 1,090 (n = 6)
Primary B cells	PI3K-δ	αIgM/CD40	10% FCS	proliferation	0.5 ± 0.16 (n = 3)
Primary T cells	PI3K-δ/γ	ConA	10% FCS	proliferation	9.5 ± 3.6 (n = 3)
Basophils	PI3K-δ	αFCεR1	whole blood	degranulation	96.1 ± 75.5 (n = 7)
Basophils	PI3K-γ	fMLP	whole blood	degranulation	1,028 ± 803 (n = 16)
Platelets	PI3K-β	thrombin peptide	whole blood	GPIIb/IIIa activation	4,700 ± 1,800 (n = 10)

ConA, concanavalin A; FCS, fetal calf serum; *f*MLP, formyl-methionyl-leucyl-phenylalanine.
See also Figure S2 and Tables S1–S3.

IPI-145 shows activity against PI3K-β biochemically and in cell-based assays. Therefore, we determined the effect of IPI-145 on PI3K-β function in platelets by using a thrombin peptide stimulus and measuring the inhibition of activated GPIIb/IIIa (Bowers et al., 2007; Jackson et al., 2005). The average IC_{50} value for IPI-145 in this PI3K-β-specific assay was 4,700 nM, indicating an ~4-fold window between PI3K-γ and PI3K-β inhibition in whole blood (Table 1).

IPI-145 Demonstrates Activity in a PI3K-γ-Dependent In Vivo Model

To characterize the ability of IPI-145 to specifically inhibit PI3K-γ in an in vivo setting, rats with previously established air pouches were dosed orally with vehicle, increasing doses of IPI-145, or the PI3K-δ-selective compound IPI-3063 (Figures 2A, 2B, and S3A; Table S4). One hour after compound dosing, blood was harvested for pharmacokinetic (PK) analysis and the pouches were injected with KC/GRO, a PI3K-γ-dependent IL-8 family chemokine (Hirsch et al., 2000; Sasaki et al., 2000). Five hours after dosing (4 hr after chemokine injection), another PK sample was taken and cells were harvested from the pouch. IPI-145 significantly inhibited neutrophil migration in the 10 and 5 mg/kg dose groups (Figure 2A), but not at the lower doses of 2.5 and 1 mg/kg. A more detailed view of the relationship between exposure and response for each animal in this model is shown in Figure 2B. All animals in the 10 mg/kg dose group showed significantly decreased neutrophil migration, whereas animals from the 5 and 2.5 mg/kg dose groups were more variable, with little inhibition at 1 mg/kg. The majority of animals with drug concentrations at or above the cellular IC_{50} value for PI3K-γ (after correction for protein binding) demonstrated reduced neutrophil influx (Figure 2B, black arrow). In contrast, all animals demonstrated IPI-145 drug levels that were ≥10-fold above the corresponding PI3K-δ cell-based IC_{50} value (Figure 2B, red arrow), implying that this effect is not mediated by PI3K-δ. To further confirm a PI3K-γ-dependent effect, IPI-3063, which has potent activity in the PI3K-δ cellular assay (IC_{50} = 0.1 nM) and limited activity toward PI3K-γ (cellular IC_{50} = 418 nM) (Table S4), was evaluated in the air pouch model. Animals were dosed with vehicle or 50 mg/kg IPI-3063 and PK samples were collected at 1 and 5 hr after dosing. At these time points, the free drug concentration (~40 nM) was >400-fold higher than the IC_{50} value in the PI3K-δ cellular assay, yet there was no significant inhibition of neutrophil migration compared with control (Figure S3B). This lack of inhibition was consistent with drug concentrations being well below the corresponding IC_{50} value of IPI-3063 in the PI3K-γ cellular assay (418 nM; Table S4). Together, these studies support the hypothesis that the KC/GRO air pouch model is primarily PI3K-γ dependent, and that inhibition of neutrophil migration by IPI-145 requires exposures consistently at or above those predicted by the corresponding PI3K-γ-dependent cellular assay IC_{50} value.

IPI-145 Is Active in a Therapeutic Rat CIA Model

We explored the therapeutic value of combined PI3K-δ and PI3K-γ blockade in inflammatory and autoimmune disease model systems. Previous studies suggested that both PI3K-δ and PI3K-γ play a role in joint inflammation associated with rheumatoid arthritis (RA) (Bartok et al., 2012; Camps et al., 2005; Randis et al., 2008); therefore, we investigated the activity of IPI-145 in an established disease version of CIA (Bendele, 2001). Reductions in ankle swelling in animals treated with IPI-145 ranged from 25% to 89% relative to vehicle controls and were statistically significant compared with vehicle, with the exception of the lowest dose (0.1 mg/kg; Figure 3A). In the same study, treatment with the TNF inhibitor etanercept (10 mg/kg) as a positive control reduced ankle diameter area under the curve (AUC) by 70% relative to vehicle (Figure 3A). To construct a relationship between plasma exposure of IPI-145 and the effect on ankle diameter, PK analysis was performed on plasma samples collected on the last day of the 7-day dosing period. Figure 3B depicts the plasma IPI-145 AUC over a 24 hr period associated with increasing doses of IPI-145 (indicated as mg/kg below the AUC markers) relative to the corresponding percent reduction in ankle diameter AUC. As can be seen, there was a moderate plateau for the reduction in ankle swelling, leading up to an AUC of ~2,000 nM*hr (5 mg/kg), with a further increase in efficacy at the highest exposure (AUC ~20,000 nM*hr at the 10 mg/kg dose). These doses correspond to the same two doses at which IPI-145 was most effective in the PI3K-γ-dependent air pouch model (Figures 2A and 2B). This dose-response correlation is consistent with the hypothesis that efficacy at lower doses in the CIA model is dependent on PI3K-δ inhibition, but for maximal efficacy, inhibition of PI3K-γ may also be required.

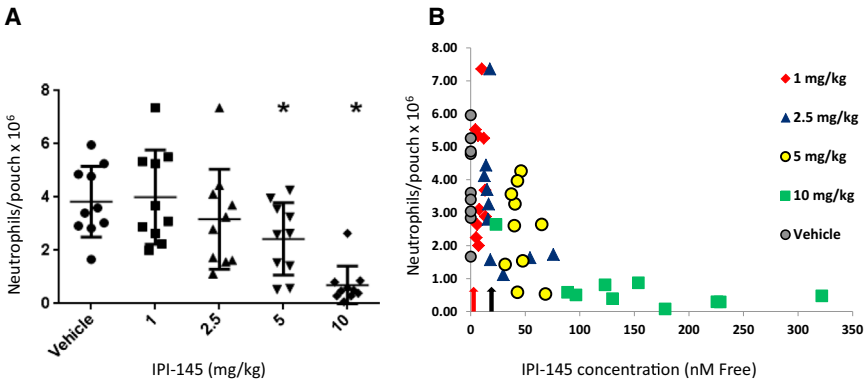

Figure 2. Effect of IPI-145 on Neutrophil Migration in a Rat Air Pouch In Vivo Model System

(A) Dose-responsive inhibition of neutrophil migration to 2.4 μg KC/GRO by IPI-145. Doses of 5 and 10 mg/kg IPI-145 are significantly different from vehicle (asterisks indicate $p < 0.05$, assessed using the Mann-Whitney nonparametric t test). Data are represented as the mean, and error bars are ±SEM. (B) Exposure-response relationship for individual animals dosed with IPI-145 in the PI3K-γ-dependent air pouch model. Each marker represents the average plasma concentration (nanomolar free based on the value of 89% protein bound for IPI-145 in rat plasma at 10 μM IPI-145) of IPI-145 taken at 1 and 5 hr after dosing versus the corresponding number of neutrophils harvested from the pouch 4 hr after KC/GRO injection. Arrows below the x axis correspond to the PI3K-δ (red) and PI3K-γ (black) cellular IC_{50}.
See also Figure S3 and Table S4.

An effect on histopathologic parameters was observed in all dose groups (Figures 3C and 3D). Significant reductions in bone/cartilage erosion and resorption and pannus formation were observed at doses > 0.1 mg/kg, whereas a reduction in cellular infiltration required higher exposures (>0.5 mg/kg). A notable further significant decrease in immune cell influx was seen at 10 mg/kg compared with 5 mg/kg (Figure 3C). This suggests an effect of PI3K-γ inhibition on cell migration at higher IPI-145 doses, similar to the observation in the air pouch model (Figures 2A and 2B).

In a parallel study to evaluate the effect of IPI-145 treatment on cytokines in rats with CIA, the levels of IL-1 and KC/GRO were measured in paw lysates from disease control and IPI-145-treated animals (5 mg/kg) on day 13. IPI-145 treatment reduced these cytokines significantly, suggesting that control of inflammatory mediators could contribute to the efficacy of IPI-145 in this model (Figure 3E).

IPI-145 Suppresses Cellular Inflammation in a Rat Model of OVA-Induced Asthma

OVA-induced asthma in rodents resembles allergic asthma and is characterized by eosinophilic lung inflammation, increased IgE production, airway hyperresponsiveness (AHR), mucus hypersecretion, and airway remodeling (Leong and Huston, 2001). Since PI3K-δ and PI3K-γ are implicated in different aspects of airway inflammation (Lee et al., 2006; Nashed et al., 2007; Takeda et al., 2009), the effect of IPI-145 in the OVA-induced asthma model was examined. IPI-145 significantly reduced eosinophils in the bronchoalveolar lavage (BAL) fluid of OVA-sensitized and -challenged animals after the 1 and 10 mg/kg doses (Figure 4A). At 10 mg/kg IPI-145, the inhibition of eosinophil infiltration was equivalent to that obtained with the positive control, 10 mg/kg dexamethasone (Figure 4A). Levels of tumor necrosis factor α (TNF-α), KC/GRO, interleukin-13 (IL-13), and IL-5 levels in the BAL were significantly suppressed following treatment with 10 mg/kg IPI-145, suggesting that reductions in these inflammatory mediators could be related to the efficacy observed in this model (Figure 4B). Histological analysis of lung tissue revealed that treatment with IPI-145 10 mg/kg markedly reduced the number and density of inflammatory cell infiltrates compared with vehicle, whereas no inflammatory lesions were observed in the dexamethasone control group (Figures 4C and 4D).

IPI-145 Is Highly Effective in the NZBWF1/J Murine Lupus Nephritis Model

NZBWF1/J mice develop a syndrome that is similar to human lupus, with the production of antinuclear and anti-double-stranded DNA (dsDNA) autoantibodies, glomerulonephritis, proteinuria, splenomegaly, lymphadenopathy, and eventually death due to kidney failure (Banham-Hall et al., 2012; Perry et al., 2011). Since both PI3K-δ and PI3K-γ have been shown to be important for the development and maintenance of lupus in mouse models (Barber et al., 2006; Maxwell et al., 2012), the efficacy of IPI-145 was evaluated in the NZBWF1/J model. By 23 weeks of age, NZBWF1/J mice began to develop increasing anti-dsDNA antibody titers (Figure 5A) and evidence of proteinuria (data not shown), indicative of kidney damage associated with lupus. Beginning at this time, animals were orally dosed daily for 20 weeks with vehicle, IPI-145 (1, 5, or 10 mg/kg), or a dexamethasone control (2 mg/kg). Proteinuria was significantly reduced at study termination for all IPI-145-treated mice compared with vehicle animals, as well as in the dexamethasone control group (Figure 5B). The effect on proteinuria was accompanied by marked reductions in anti-dsDNA autoantibody production at 5 or 10 mg/kg (Figure 5A), but not at the 1 mg/kg dose level, indicating that diminished kidney damage is not solely related to reductions in anti-dsDNA titers. Histopathologic evaluation confirmed the clinical observations, with the summation of kidney histopathology parameters (summed scores of histopathologic assessment of glomerulonephritis, interstitial nephritis, vessel inflammation, and protein casts) being significantly reduced for mice treated with IPI-145 in a dose-dependent manner (Figure 5C).

DISCUSSION

PI3K-δ and PI3K-γ isoforms are preferentially expressed in leukocytes, where they have distinct and nonoverlapping roles in immune cell function (Bone and Welham, 2007; Burger and Hoellenriegel, 2011; Cushing et al., 2012; Hoellenriegel et al., 2011;

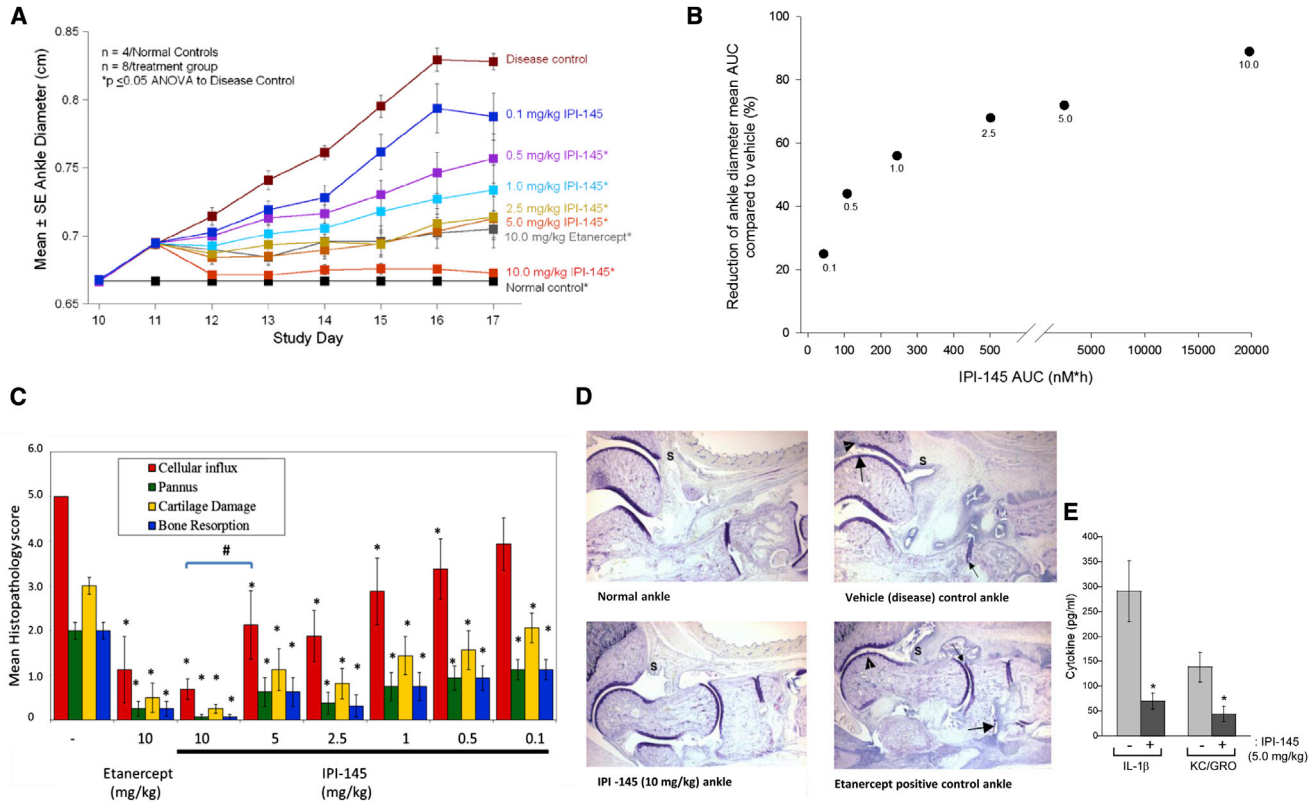

Figure 3. Activity of IPI-145 in a Rat CIA Model

(A) Dose-responsive decrease in mean ankle diameter by IPI-145 in the rat CIA model. All groups of IPI-145-treated animals are significantly different from diseased (vehicle) control from day 11 to day 17, with the exception of 0.1 mg/kg IPI-145.

(B) IPI-145 levels (AUC) versus efficacy plot for the CIA study shown in (A). Corresponding IPI-145 dose levels are noted below each data point.

(C) Histopathology scoring (0 = normal, 5 = most severe) for ankles, showing dose-responsive control of disease. Histopathology includes separate scores for cellular influx, pannus, cartilage damage, and bone resorption. The asterisk (*) denotes significance compared with vehicle control. The # symbol denotes significant differences in cellular influx scores between 5 mg/kg and 10 mg/kg IPI-145-treated groups.

(D) Representative ankle photomicrographs from animals with the approximate mean group score from normal, vehicle (disease) control, 10 mg/kg IPI-145, and 10 mg/kg etanercept positive control animals. Cartilage and pannus are indicated by large and small arrows, respectively, and bone resorption is indicated by an arrowhead. S, synovium.

(E) Effect of IPI-145 treatment on proinflammatory cytokines. Ankle lysates (five animals per group) from disease control or 5 mg/kg IPI-145-treated rats were analyzed at day 13 for IL-1 and KC/GRO by Meso Scale Discovery (*$p < 0.05$ versus disease control).

Data are represented as the mean, and error bars are ±SEM. This experiment is representative of seven replicate experiments.

Lannutti et al., 2011; Puri and Gold, 2012; Subramaniam et al., 2012; Winer et al., 2012). Given these key roles, inhibitors of these isoforms have been postulated to have therapeutic potential in immune-related inflammatory or hematologic diseases (Williams et al., 2010). Here, we have described IPI-145, a molecule that potently inhibits PI3K-δ with a biochemical IC_{50} of 2.5 nM, a cellular IC_{50} in the subnanomolar range, and a whole-blood IC_{50} of ~100 nM. IPI-145 also has activity against PI3K-γ, with IC_{50} values at concentrations that are ~10-fold higher than the IC_{50} values for PI3K-δ. This property makes it possible to increasingly suppress PI3K-γ activity with higher concentrations of IPI-145 while continuously maintaining PI3K-δ inhibition. Inhibition of PI3K-β equivalent to that of PI3K-γ would require even greater concentrations of IPI-145. Early clinical investigations with IPI-145 in patients with certain hematologic malignancies demonstrated activity at doses in a range that showed significant inhibition (>IC_{50}) of PI3K-δ and PI3K-γ, but below the IC_{50} for PI3K-β (Patel et al., 2013; Flinn et al., 2012).

Human leukocyte in vitro cellular assays and rodent in vivo studies have demonstrated that IPI-145 exerts effects on the adaptive and innate immune response by inhibiting B and T cell proliferation, blocking neutrophil migration, and reducing basophil activation. The ability of IPI-145 to inhibit both PI3K-δ and PI3K-γ simultaneously in a single cell is of particular importance. Given the interdependence of these pathways in immune cell function, the combined effect of this dual inhibition can lead to an enhanced anti-inflammatory effect compared with inhibition of one isoform alone (Williams et al., 2010). IPI-145 demonstrated therapeutic activity in three separate rodent inflammatory disease models: (1) a rat CIA model in which IPI-145 inhibited ankle swelling, inflammation, joint damage, and bone destruction; (2) a rat OVA-induced asthma model in which dose-responsive reduction of pulmonary inflammation and eosinophilia were observed; and (3) a spontaneous murine systemic lupus erythematosus model in which IPI-145 was associated with reductions in

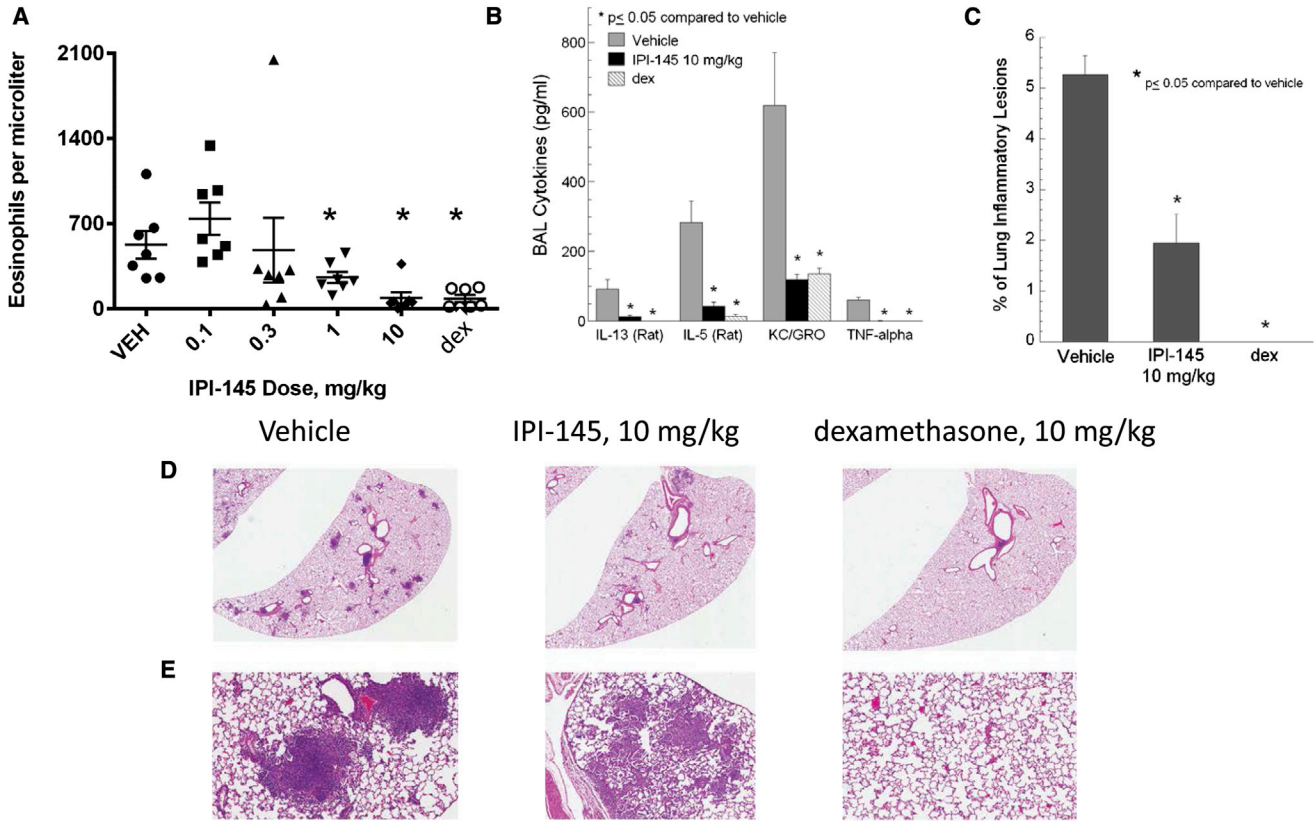

Figure 4. Anti-Inflammatory Effects of IPI-145 in the Rat OVA-Induced Asthma Model

(A) Effect of IPI-145 on eosinophil infiltration measured in BAL fluid in the rat OVA-induced asthma model.

(B) Effect of IPI-145 treatment on inflammatory cytokine production measured in BAL fluid in rats with OVA-induced asthma.

(C) Quantification of lung inflammatory lesions. Lungs from three animals from each group (vehicle, 10 mg/kg IPI-145, and 10 mg/kg dexamethasone) that were not lavaged were fixed and stained for histological analysis.

(D) Low-power view of lung tissue.

(E) High-power view of lung tissue, focusing on inflammatory infiltrate.

Data are represented as the mean, and error bars are ±SEM. This experiment is representative of two replicate experiments.

anti-dsDNA antibody titers and resolution of proteinuria and glomerulonephritis.

PI3K-δ and PI3K-γ are proximal in the signal transduction cascades utilized by the adaptive immune system, including B cell and T cell receptor, Fc receptor, growth factor receptor, and chemokine and cytokine receptor pathways. For innate immune cells, these PI3K isoforms are involved in toll-like receptor signaling and mediate chemokine and cytokine signaling and production (Durand et al., 2009; Guiducci et al., 2008). IPI-145 will thus disrupt both adaptive and innate immune arms, leading to efficacy in inflammatory disease models.

This is particularly true in RA models, where the importance of both PI3K-δ and PI3K-γ in disease pathogenesis has been clearly established (Camps et al., 2005; Randis et al., 2008). In a serum-induced arthritis model system, PI3K-δ genetic deletion or pharmacological inhibition diminished joint erosion to a level comparable to that observed with the PI3K-γ-deficient counterpart. However, the induction and progression of joint destruction were most potently reduced in the absence of both PI3K isoforms (Randis et al., 2008). A role for PI3K-δ in human inflammatory RA synoviocyte migration and other functions was recently reported, suggesting another disease mechanism affected by the PI3K-δ pathway (Bartok et al., 2012). Additionally, investigators employing a collagen antibody-induced arthritis model demonstrated that genetic deletion of PI3K-γ protected mice against disease development and reduced neutrophil infiltrates in joints when compared with PI3K-γ wild-type animals (Camps et al., 2005).

In the CIA model, plasma exposures of IPI-145 above 100 nM*hr (achieved at a dose ≥ 0.5 mg/kg) led to a significant reduction in the degree of joint swelling in established CIA, consistent with inhibition of PI3K-δ playing a key role in this effect. In addition, pannus, cartilage damage, and bone resorption were all significantly decreased with IPI-145, even at the lowest dose level (0.1 mg/kg). Importantly, enhanced reductions in joint swelling, beyond that seen with etanercept at 10 mg/kg, were observed when IPI-145 plasma exposures were above 2,000 nM*hr, which is consistent with the additive effect of IPI-145-mediated inhibition of PI3K-γ. The ability of IPI-145 to inhibit neutrophil migration through PI3K-γ blockade may play an additional key role in the efficacy of IPI-145 in this model system, as was demonstrated directly in the rat air pouch model. In this model, KC/GRO-induced neutrophil influx was blocked by

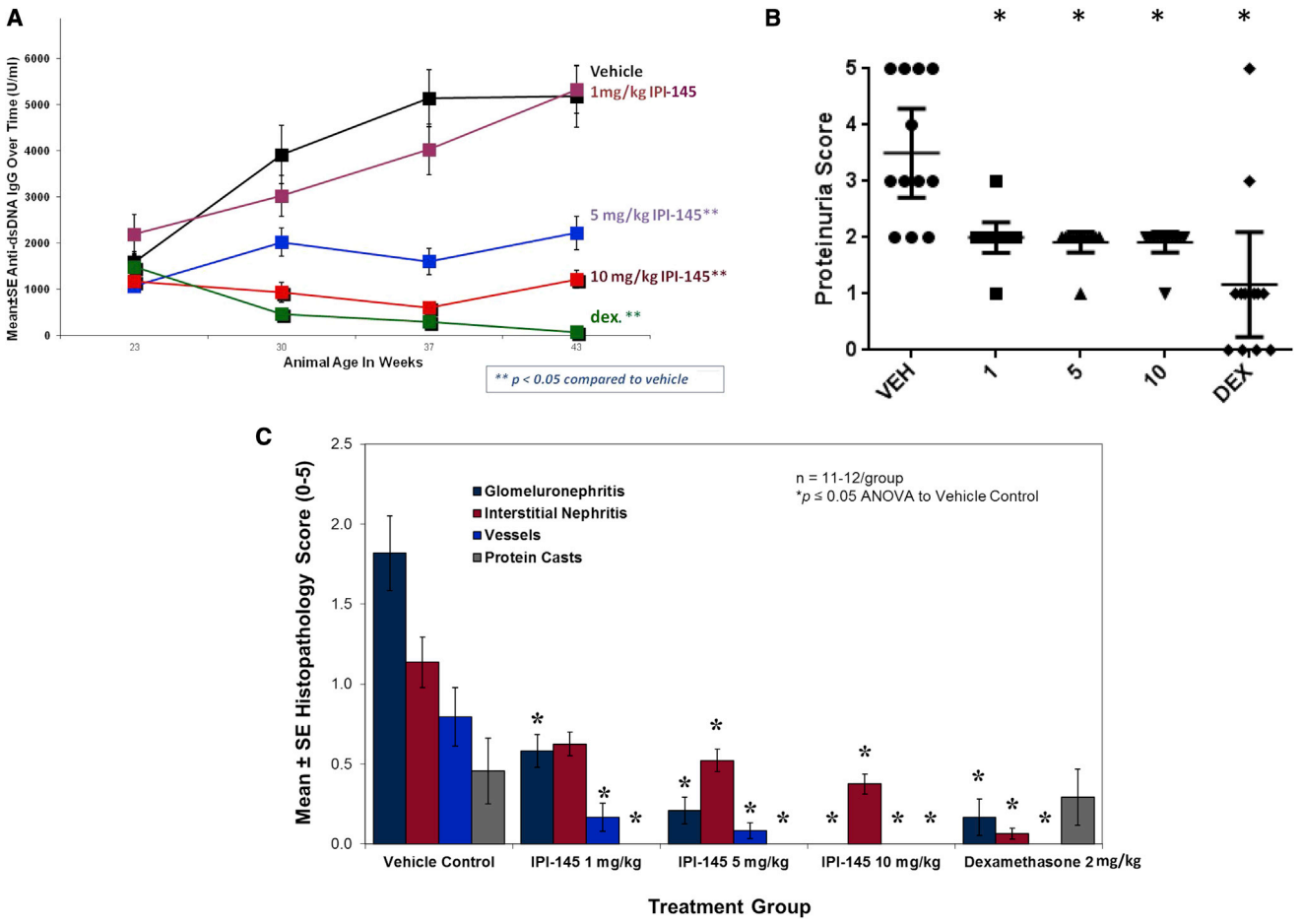

Figure 5. Therapeutic Effects of IPI-145 in the NZBWF1/J Murine Model of Systemic Lupus Erythematosus Nephritis

Effects in mice treated with IPI-145 (1, 5, and 10 mg/kg), dexamethasone (2 mg/kg), or vehicle.

(A) Anti-dsDNA titers.

(B) Proteinuria at study termination (43 weeks).

(C) Histopathological assessment of kidneys (glomerulonephritis, interstitial nephritis, vessels, and protein casts) at study termination (*p < 0.05, assessed using ANOVA compared with vehicle control).

Data are represented as the mean, and error bars are ±SEM. This study has been completed once.

IPI-145 at doses of 5 or 10 mg/kg, which correspond to free drug concentrations above the cellular IC_{50} value for PI3K-γ. These findings are pharmacologic confirmation that neutrophil migration in response to KC/GRO is PI3K-γ dependent. Genetic studies also corroborate the concept that promigratory signaling through CXCR2 (the KC/GRO receptor) is PI3K-γ dependent (Hirsch et al., 2000; Sasaki et al., 2000). Further support for the notion that neutrophil trafficking is dependent on PI3K-γ, but not PI3K-δ, comes from the finding that the PI3K-δ-selective inhibitor IPI-3063 does not block neutrophil migration at concentrations where complete inhibition of only PI3K-δ is expected. Therefore, the enhanced inhibitory effect on cellular infiltration into ankle joints with high concentrations of IPI-145 (e.g., 10 mg/kg versus lower doses) in the CIA model is consistent with greater PI3K-γ inhibition of cell migration. The inhibition of neutrophil migration, lymphocyte proliferation, and mast cell activation (Table 1; Figure S2) likely contribute to the significant therapeutic effect of combined PI3K-γ and PI3K-δ inhibition in this model of RA.

Small-molecule inhibitors of inflammatory pathways are actively being investigated for RA therapy. Inhibitors of BTK and SYK, which signal in conjunction with PI3K-δ, as well as JAK kinases, have been evaluated preclinically in RA models. The most advanced of these inhibitors is tofacitinib, a recently approved pan-JAK inhibitor (Chakravarty et al., 2013). Based on preclinical data comparisons, the in-life efficacy and protection from joint damage seen histologically with IPI-145 in the rat CIA model is equivalent to that demonstrated with tofacitinib in the murine CIA model (Milici et al., 2008).

In the rat OVA-induced asthma model, IPI-145, at levels where combined PI3K-δ and PI3K-γ inhibition is achieved, demonstrated potent, dose-dependent inhibition of the alveolar influx of eosinophils and inhibited granulocyte influx to the same extent as dexamethasone (Figure 4A). In addition, IPI-145 suppressed key inflammatory mediators such as IL-13, IL-5, KC/GRO, and TNF-α as potently as dexamethasone (Figure 4B). The therapeutic potential for PI3K inhibition in respiratory disease has been demonstrated by the resistance of PI3K-δ− and PI3K-γ-deficient

mice to disease in models of OVA-induced asthma (Lee et al., 2006; Nashed et al., 2007; Takeda et al., 2009). In addition, the effects of PI3K-δ inhibitors on the cigarette-smoke-induced model of chronic obstructive pulmonary disease and smooth muscle AHR suggest a broader role for PI3K-δ inhibitors in respiratory diseases (Ge et al., 2012).

Finally, in the murine NZB/W F1 model of lupus nephritis, IPI-145 demonstrated dose-responsive kidney protection compared with control at all doses administered (1, 5, and 10 mg/kg). In this model system, efficacy has been demonstrated with therapeutics that affect the adaptive immune pathways responsible for plasma cell differentiation and survival, as well as those that block innate immune pathways leading to interferon response (Neubert et al., 2008). With IPI-145, dose-responsive reduction of anti-dsDNA autoantibodies occurred with 5 and 10 mg/kg. Interestingly, a lower dose of IPI-145 (1 mg/kg) was able to protect the kidney (as demonstrated by reduced proteinuria) even though it did not decrease autoimmunity as measured by specific autoantibody levels. This suggests that protection in this model may be afforded by more than one PI3K-dependent pathway. PI3K-δ plays a role in toll-like receptor signaling leading to type 1 interferon production, and inhibition of this pathway may contribute to the efficacy seen with IPI-145 in this model (Guiducci et al., 2008). PI3K-δ reduction (gene deletion heterozygotes) or deletion (homozygotes) is protective in an autoimmune lupus model, suggesting that even partial inhibition of this enzyme may be therapeutic. PI3K-γ inhibition is also protective in lupus models, and inhibition of this isoform may contribute to the efficacy observed with higher doses of IPI-145 (Maxwell et al., 2012).

Since PI3K signaling controls B and T cell proliferation and survival, the lymphocyte-specific isoforms PI3K-δ and PI3K-γ have also been exploited by hematopoietic cancers, including chronic lymphocytic leukemia (CLL), acute myeloid leukemia (AML), and non-Hodgkin's lymphoma (NHL) (Billottet et al., 2006). In T cell acute lymphoblastic leukemia (T-ALL), activation of the PI3K pathway is a common event, and inhibition or deletion of both PI3K-δ and PI3K-γ, but not single isoforms, was shown to be therapeutic in a murine disease model (Subramaniam et al., 2012). A PI3K-δ inhibitor, GS-1101, is currently under clinical development for use in hematologic malignancies as a single agent and in combination with other cytotoxic therapies (Lannutti et al., 2011). In addition, early phase 1 clinical data suggest that IPI-145 is well tolerated and clinically active in patients with advanced hematologic malignancies (Flinn et al., 2012). Preliminary results indicate that clinical activity was observed in a wide variety of B and T cell NHLs, CLL, and Hodgkin lymphoma, supporting the hypothesis that both B cell and T cell malignancies are sensitive to PI3K-δ and PI3K-γ inhibition.

In summary, IPI-145 is a potent oral inhibitor of PI3K-δ and PI3K-γ, the isoforms that are predominantly expressed in immune cells. The broad spectrum of IPI-145's effects against cells of the adaptive and innate immune system translates into significant efficacy in a variety of rodent inflammatory and autoimmune disease models. Activity against PI3K-γ, with exposures that are achievable in vivo, distinguishes IPI-145 from previously described PI3K-δ-selective inhibitors. Based on these studies, clinical exploration of IPI-145 in inflammatory and autoimmune disease and hematologic malignancies is merited.

SIGNIFICANCE

IPI-145 is a potent oral class I PI3K inhibitor that targets PI3K-δ and PI3K-γ, has a K_D for these isoforms in the picomolar range, and employs an optimized single-step binding mechanism. PI3K-δ and PI3K-γ isoforms are preferentially expressed in leukocytes, where they have distinct and nonoverlapping roles in immune cell development and function. As key enzymes in leukocyte signaling, PI3K-δ and PI3K-γ facilitate normal lymphoid (B and T cells) and myeloid cell functions, including differentiation, activation, and migration. Preclinical models of autoimmune and inflammatory diseases demonstrate the critical role of PI3K-δ and/or PI3K-γ activity in their pathophysiology. IPI-145 has profound effects on adaptive and innate immune cell function and is therapeutic in animal models of inflammatory and autoimmune disease. In immune-mediated diseases, as well as cancers of the immune system, IPI-145 has a unique therapeutic potential that is currently being explored in clinical trials. IPI-145 is being pursued in clinical trials for various hematologic malignancies (ClinicalTrials.gov identifiers: NCT01476657, NCT01882803, and NCT01871675) and inflammatory diseases, such as asthma (NCT01653756) and RA (NCT01851707).

EXPERIMENTAL PROCEDURES

Reagents

IPI-145 was prepared in our laboratories using methods described in U.S. Patent 8,193,182. IPI-3063 was prepared in our laboratories using methods described in patent application WO2013032591. Small-molecule inhibitors were stored as a 10 mM stock solution in DMSO at room temperature. All human PI3K isoform proteins were purchased from Millipore. Radiolabeled [α-^{32}P] ATP was purchased from Perkin Elmer with a specific activity of 800 Ci/mmol. Phosphatidylinositol 4,5 bis phosphate (diC$_8$-PIP$_2$) was purchased from Avanti Polar Lipids. For dissociation studies, [^{3}H]IPI-145 was custom synthesized at Ambios Labs. The dissociation studies are described in Supplemental Experimental Procedures.

Primary Human B and T Cell Proliferation Assays

Human peripheral blood CD19$^+$ B cells and CD3$^+$ T cells were purchased from Allcells and proliferation assays were conducted as described in Supplemental Experimental Procedures.

Basophil Activation Assay

Evaluation of basophil function was performed using the FlowCast basophil activation test (Bulmann Laboratories) according to the manufacturer's instructions, as described in Supplemental Experimental Procedures.

Platelet Activation Assay

The platelet activation assay was conducted as described in Supplemental Experimental Procedures.

Air Pouch Model of Cell Migration

Female Wistar rats were obtained from Charles River Laboratories. All in vivo research was conducted in accordance with the Guide for the Care and Use of Laboratory Animals published by the National Research Council of the National Academies and under the approval of the Institutional Animal Care and Use Committee. On day 0, the rats were anesthetized, their backs were shaved, and pouches were generated by a subcutaneous injection of 20 ml sterile air filtered through a 0.2 μm filter. On day 3, the pouches were reinflated with 10 ml of sterile air. On day 6, the rats were dosed orally with either test compound or vehicle. One hour after dosing, rats were anesthetized and blood was collected in EDTA tubes. Following blood collection, 2.4 μg of

recombinant rat KC/GRO (Peprotech) in 2 ml of endotoxin-free water or water alone (Teknova) was injected into the pouch. Four hours after KC/GRO stimulation, the rats were euthanized and bled via cardiac puncture. Pouches were washed with 5 ml of cold PBS (Teknova) and 4 ml of exudate was collected from each pouch. Differential cell counts were measured using a CELL-DYN 3700 instrument (Abbott). Data were analyzed using Graphpad Prism software.

Induction of Rat Arthritis by Type II Collagen

Female Lewis rats weighing 125–150 g were used for the induction of arthritis (Bendele, 2001). CIA studies are described in detail in Supplemental Experimental Procedures.

Evaluation of IPI-145 in the Rat OVA-Induced Asthma Model

Rat OVA-induced asthma studies were performed at Charles River Labs as described in Supplemental Experimental Procedures.

NZBWF1/J Model of Systemic Lupus Erythematosus Nephritis

Studies of the NZBWF1/J model of systemic lupus erythematosus nephritis were performed at Bolder BioPATH as described in Supplemental Experimental Procedures.

SUPPLEMENTAL INFORMATION

Supplemental Information includes Supplemental Experimental Procedures, three figures, and four tables and can be found with this article online at http://dx.doi.org/10.1016/j.chembiol.2013.09.017.

AUTHOR CONTRIBUTIONS

J.R.M., A.R.L., J.P.D., E.E.B., M.P., J.L.P., C.R.M., J.G.H., B.T., E.L.M., B.D.T., P.R., Y.L., L-S.L., K.A.J., and D.G.W. designed, coordinated, and performed the experiments. D.G.W., K.L.F., J.R.M., C.C.F., C.R., J.R.P., V.J.P., J.L.D., P.S.C., J.A.A., and J.L.K. were involved in data analysis and interpretation. D.G.W., C.C.F., P.S.C., and J.L.K. wrote the paper with input from all coauthors.

ACKNOWLEDGMENTS

We thank Karen D'Amour for invaluable assistance with manuscript preparation. At the time this work was done, the authors were employees and shareholders of Infinity Pharmaceuticals, Inc., or Intellikine, Inc.

Received: June 7, 2013
Revised: September 6, 2013
Accepted: September 18, 2013
Published: November 7, 2013

REFERENCES

Al-Alwan, M.M., Okkenhaug, K., Vanhaesebroeck, B., Hayflick, J.S., and Marshall, A.J. (2007). Requirement for phosphoinositide 3-kinase p110delta signaling in B cell antigen receptor-mediated antigen presentation. J. Immunol. *178*, 2328–2335.

Banham-Hall, E., Clatworthy, M.R., and Okkenhaug, K. (2012). The therapeutic potential for PI3K inhibitors in autoimmune rheumatic diseases. Open Rheumatol. J. *6*, 245–258.

Barber, D.F., Bartolomé, A., Hernandez, C., Flores, J.M., Fernandez-Arias, C., Rodríguez-Borlado, L., Hirsch, E., Wymann, M., Balomenos, D., and Carrera, A.C. (2006). Class IB-phosphatidylinositol 3-kinase (PI3K) deficiency ameliorates IA-PI3K-induced systemic lupus but not T cell invasion. J. Immunol. *176*, 589–593.

Bartok, B., Boyle, D.L., Liu, Y., Ren, P., Ball, S.T., Bugbee, W.D., Rommel, C., and Firestein, G.S. (2012). PI3 kinase δ is a key regulator of synoviocyte function in rheumatoid arthritis. Am. J. Pathol. *180*, 1906–1916.

Bendele, A. (2001). Animal models of rheumatoid arthritis. J. Musculoskelet. Neuronal Interact. *1*, 377–385.

Bi, L., Okabe, I., Bernard, D.J., Wynshaw-Boris, A., and Nussbaum, R.L. (1999). Proliferative defect and embryonic lethality in mice homozygous for a deletion in the p110alpha subunit of phosphoinositide 3-kinase. J. Biol. Chem. *274*, 10963–10968.

Bilancio, A., Okkenhaug, K., Camps, M., Emery, J.L., Ruckle, T., Rommel, C., and Vanhaesebroeck, B. (2006). Key role of the p110delta isoform of PI3K in B-cell antigen and IL-4 receptor signaling: comparative analysis of genetic and pharmacologic interference with p110delta function in B cells. Blood *107*, 642–650.

Billottet, C., Grandage, V.L., Gale, R.E., Quattropani, A., Rommel, C., Vanhaesebroeck, B., and Khwaja, A. (2006). A selective inhibitor of the p110delta isoform of PI 3-kinase inhibits AML cell proliferation and survival and increases the cytotoxic effects of VP16. Oncogene *25*, 6648–6659.

Bone, H.K., and Welham, M.J. (2007). Phosphoinositide 3-kinase signalling regulates early development and developmental haemopoiesis. J. Cell Sci. *120*, 1752–1762.

Bowers, R.K., Marder, P., Green, L.J., Horn, C.L., Faber, A.L., and Thomas, J.E. (2007). A platelet biomarker for assessing phosphoinositide 3-kinase inhibition during cancer chemotherapy. Mol. Cancer Ther. *6*, 2600–2607.

Burger, J.A., and Hoellenriegel, J. (2011). Phosphoinositide 3′-kinase delta: turning off BCR signaling in chronic lymphocytic leukemia. Oncotarget *2*, 737–738.

Camps, M., Rückle, T., Ji, H., Ardissone, V., Rintelen, F., Shaw, J., Ferrandi, C., Chabert, C., Gillieron, C., Françon, B., et al. (2005). Blockade of PI3Kgamma suppresses joint inflammation and damage in mouse models of rheumatoid arthritis. Nat. Med. *11*, 936–943.

Chakravarty, S.D., Poulikakos, P.I., Ivashkiv, L.B., Salmon, J.E., and Kalliolias, G.D. (2013). Kinase inhibitors: a new tool for the treatment of rheumatoid arthritis. Clin. Immunol. *148*, 66–78.

Clayton, E., Bardi, G., Bell, S.E., Chantry, D., Downes, C.P., Gray, A., Humphries, L.A., Rawlings, D., Reynolds, H., Vigorito, E., and Turner, M. (2002). A crucial role for the p110delta subunit of phosphatidylinositol 3-kinase in B cell development and activation. J. Exp. Med. *196*, 753–763.

Condliffe, A.M., Davidson, K., Anderson, K.E., Ellson, C.D., Crabbe, T., Okkenhaug, K., Vanhaesebroeck, B., Turner, M., Webb, L., Wymann, M.P., et al. (2005). Sequential activation of class IB and class IA PI3K is important for the primed respiratory burst of human but not murine neutrophils. Blood *106*, 1432–1440.

Cushing, T.D., Metz, D.P., Whittington, D.A., and McGee, L.R. (2012). PI3Kδ and PI3Kγ as targets for autoimmune and inflammatory diseases. J. Med. Chem. *55*, 8559–8581.

Dil, N., and Marshall, A.J. (2009). Role of phosphoinositide 3-kinase p110 delta in TLR4- and TLR9-mediated B cell cytokine production and differentiation. Mol. Immunol. *46*, 1970–1978.

Durand, C.A., Hartvigsen, K., Fogelstrand, L., Kim, S., Iritani, S., Vanhaesebroeck, B., Witztum, J.L., Puri, K.D., and Gold, M.R. (2009). Phosphoinositide 3-kinase p110 delta regulates natural antibody production, marginal zone and B-1 B cell function, and autoantibody responses. J. Immunol. *183*, 5673–5684.

Flinn, I., Horwitz, S., Patel, M., Younes, A., Porter, J., Sweeney, J., Allen, K., Kelly, P., and Kahl, B. (2012). Clinical safety and activity in a phase 1 trial of IPI-145, a potent inhibitor of phosphoinositide-3-kinase-d,g, in patients with advanced hematologic malignancies. Blood (ASH Annual Meeting Abstracts) *120*, 3663.

Garçon, F., Patton, D.T., Emery, J.L., Hirsch, E., Rottapel, R., Sasaki, T., and Okkenhaug, K. (2008). CD28 provides T-cell costimulation and enhances PI3K activity at the immune synapse independently of its capacity to interact with the p85/p110 heterodimer. Blood *111*, 1464–1471.

Ge, Q., Moir, L.M., Trian, T., Niimi, K., Poniris, M., Shepherd, P.R., Black, J.L., Oliver, B.G., and Burgess, J.K. (2012). The phosphoinositide 3′-kinase p110δ modulates contractile protein production and IL-6 release in human airway smooth muscle. J. Cell. Physiol. *227*, 3044–3052.

Guiducci, C., Ghirelli, C., Marloie-Provost, M.A., Matray, T., Coffman, R.L., Liu, Y.J., Barrat, F.J., and Soumelis, V. (2008). PI3K is critical for the nuclear

translocation of IRF-7 and type I IFN production by human plasmacytoid predendritic cells in response to TLR activation. J. Exp. Med. *205*, 315–322.

Haylock-Jacobs, S., Comerford, I., Bunting, M., Kara, E., Townley, S., Klingler-Hoffmann, M., Vanhaesebroeck, B., Puri, K.D., and McColl, S.R. (2011). PI3Kδ drives the pathogenesis of experimental autoimmune encephalomyelitis by inhibiting effector T cell apoptosis and promoting Th17 differentiation. J. Autoimmun. *36*, 278–287.

Hirsch, E., Katanaev, V.L., Garlanda, C., Azzolino, O., Pirola, L., Silengo, L., Sozzani, S., Mantovani, A., Altruda, F., and Wymann, M.P. (2000). Central role for G protein-coupled phosphoinositide 3-kinase gamma in inflammation. Science *287*, 1049–1053.

Hoellenriegel, J., Meadows, S.A., Sivina, M., Wierda, W.G., Kantarjian, H., Keating, M.J., Giese, N., O'Brien, S., Yu, A., Miller, L.L., et al. (2011). The phosphoinositide 3′-kinase delta inhibitor, CAL-101, inhibits B-cell receptor signaling and chemokine networks in chronic lymphocytic leukemia. Blood *118*, 3603–3612.

Jackson, S.P., Schoenwaelder, S.M., Goncalves, I., Nesbitt, W.S., Yap, C.L., Wright, C.E., Kenche, V., Anderson, K.E., Dopheide, S.M., Yuan, Y., et al. (2005). PI 3-kinase p110beta: a new target for antithrombotic therapy. Nat. Med. *11*, 507–514.

Jou, S.T., Carpino, N., Takahashi, Y., Piekorz, R., Chao, J.R., Carpino, N., Wang, D., and Ihle, J.N. (2002). Essential, nonredundant role for the phosphoinositide 3-kinase p110delta in signaling by the B-cell receptor complex. Mol. Cell. Biol. *22*, 8580–8591.

Konrad, S., Ali, S.R., Wiege, K., Syed, S.N., Engling, L., Piekorz, R.P., Hirsch, E., Nürnberg, B., Schmidt, R.E., and Gessner, J.E. (2008). Phosphoinositide 3-kinases gamma and delta, linkers of coordinate C5a receptor-Fcgamma receptor activation and immune complex-induced inflammation. J. Biol. Chem. *283*, 33296–33303.

Kulkarni, S., Sitaru, C., Jakus, Z., Anderson, K.E., Damoulakis, G., Davidson, K., Hirose, M., Juss, J., Oxley, D., Chessa, T.A., et al. (2011). PI3Kβ plays a critical role in neutrophil activation by immune complexes. Sci. Signal. *4*, ra23.

Lannutti, B.J., Meadows, S.A., Herman, S.E., Kashishian, A., Steiner, B., Johnson, A.J., Byrd, J.C., Tyner, J.W., Loriaux, M.M., Deininger, M., et al. (2011). CAL-101, a p110delta selective phosphatidylinositol-3-kinase inhibitor for the treatment of B-cell malignancies, inhibits PI3K signaling and cellular viability. Blood *117*, 591–594.

Lee, K.S., Lee, H.K., Hayflick, J.S., Lee, Y.C., and Puri, K.D. (2006). Inhibition of phosphoinositide 3-kinase delta attenuates allergic airway inflammation and hyperresponsiveness in murine asthma model. FASEB J. *20*, 455–465.

Leong, K.P., and Huston, D.P. (2001). Understanding the pathogenesis of allergic asthma using mouse models. Ann. Allergy Asthma Immunol. *87*, 96–109, quiz 110.

Liu, L., Puri, K.D., Penninger, J.M., and Kubes, P. (2007). Leukocyte PI3Kgamma and PI3Kdelta have temporally distinct roles for leukocyte recruitment in vivo. Blood *110*, 1191–1198.

Maxwell, M.J., Tsantikos, E., Kong, A.M., Vanhaesebroeck, B., Tarlinton, D.M., and Hibbs, M.L. (2012). Attenuation of phosphoinositide 3-kinase δ signaling restrains autoimmune disease. J. Autoimmun. *38*, 381–391.

Milici, A.J., Kudlacz, E.M., Audoly, L., Zwillich, S., and Changelian, P. (2008). Cartilage preservation by inhibition of Janus kinase 3 in two rodent models of rheumatoid arthritis. Arthritis Res. Ther. *10*, R14.

Nashed, B.F., Zhang, T., Al-Alwan, M., Srinivasan, G., Halayko, A.J., Okkenhaug, K., Vanhaesebroeck, B., Hayglass, K.T., and Marshall, A.J. (2007). Role of the phosphoinositide 3-kinase p110delta in generation of type 2 cytokine responses and allergic airway inflammation. Eur. J. Immunol. *37*, 416–424.

Neubert, K., Meister, S., Moser, K., Weisel, F., Maseda, D., Amann, K., Wiethe, C., Winkler, T.H., Kalden, J.R., Manz, R.A., and Voll, R.E. (2008). The proteasome inhibitor bortezomib depletes plasma cells and protects mice with lupus-like disease from nephritis. Nat. Med. *14*, 748–755.

Okkenhaug, K., Bilancio, A., Farjot, G., Priddle, H., Sancho, S., Peskett, E., Pearce, W., Meek, S.E., Salpekar, A., Waterfield, M.D., et al. (2002). Impaired B and T cell antigen receptor signaling in p110delta PI 3-kinase mutant mice. Science *297*, 1031–1034.

Okkenhaug, K., Patton, D.T., Bilancio, A., Garçon, F., Rowan, W.C., and Vanhaesebroeck, B. (2006). The p110delta isoform of phosphoinositide 3-kinase controls clonal expansion and differentiation of Th cells. J. Immunol. *177*, 5122–5128.

Patel, M., Kahl, B., Horwitz, S., Younes, A., Foss, F., Oki, Y., Sweeney, J., Allen, K., Faia, K., Kelly, P., et al. (2013). Preliminary safety and efficacy of IPI-145, a potent inhibitor of phosphoinositide-3-kinase-δ,γ in patients with relapsed/refractory CLL. J. Clin. Oncol. (ASCO Annual Meeting Abstracts) *1*, 7070.

Perry, D., Sang, A., Yin, Y., Zheng, Y.Y., and Morel, L. (2011). Murine models of systemic lupus erythematosus. J. Biomed. Biotechnol. *2011*, 271694.

Pinho, V., Russo, R.C., Amaral, F.A., de Sousa, L.P., Barsante, M.M., de Souza, D.G., Alves-Filho, J.C., Cara, D.C., Hayflick, J.S., Rommel, C., et al. (2007). Tissue- and stimulus-dependent role of phosphatidylinositol 3-kinase isoforms for neutrophil recruitment induced by chemoattractants in vivo. J. Immunol. *179*, 7891–7898.

Puri, K.D., and Gold, M.R. (2012). Selective inhibitors of phosphoinositide 3-kinase delta: modulators of B-cell function with potential for treating autoimmune inflammatory diseases and B-cell malignancies. Front. Immunol. *3*, 256.

Randis, T.M., Puri, K.D., Zhou, H., and Diacovo, T.G. (2008). Role of PI3Kdelta and PI3Kgamma in inflammatory arthritis and tissue localization of neutrophils. Eur. J. Immunol. *38*, 1215–1224.

Roller, A., Perino, A., Dapavo, P., Soro, E., Okkenhaug, K., Hirsch, E., and Ji, H. (2012). Blockade of phosphatidylinositol 3-kinase PI3Kδ or PI3Kγ reduces IL-17 and ameliorates imiquimod-induced psoriasis-like dermatitis. J. Immunol. *189*, 4612–4620.

Sasaki, T., Irie-Sasaki, J., Jones, R.G., Oliveira-dos-Santos, A.J., Stanford, W.L., Bolon, B., Wakeham, A., Itie, A., Bouchard, D., Kozieradzki, I., et al. (2000). Function of PI3Kgamma in thymocyte development, T cell activation, and neutrophil migration. Science *287*, 1040–1046.

Schmid, M.C., Avraamides, C.J., Dippold, H.C., Franco, I., Foubert, P., Ellies, L.G., Acevedo, L.M., Manglicmot, J.R., Song, X., Wrasidlo, W., et al. (2011). Receptor tyrosine kinases and TLR/IL1Rs unexpectedly activate myeloid cell PI3kγ, a single convergent point promoting tumor inflammation and progression. Cancer Cell *19*, 715–727.

Soond, D.R., Bjørgo, E., Moltu, K., Dale, V.Q., Patton, D.T., Torgersen, K.M., Galleway, F., Twomey, B., Clark, J., Gaston, J.S., et al. (2010). PI3K p110delta regulates T-cell cytokine production during primary and secondary immune responses in mice and humans. Blood *115*, 2203–2213.

Subramaniam, P.S., Whye, D.W., Efimenko, E., Chen, J., Tosello, V., De Keersmaecker, K., Kashishian, A., Thompson, M.A., Castillo, M., Cordon-Cardo, C., et al. (2012). Targeting nonclassical oncogenes for therapy in T-ALL. Cancer Cell *21*, 459–472.

Takeda, M., Ito, W., Tanabe, M., Ueki, S., Kato, H., Kihara, J., Tanigai, T., Chiba, T., Yamaguchi, K., Kayaba, H., et al. (2009). Allergic airway hyperresponsiveness, inflammation, and remodeling do not develop in phosphoinositide 3-kinase gamma-deficient mice. J. Allergy Clin. Immunol. *123*, 805–812.

Williams, O., Houseman, B.T., Kunkel, E.J., Aizenstein, B., Hoffman, R., Knight, Z.A., and Shokat, K.M. (2010). Discovery of dual inhibitors of the immune cell PI3Ks p110delta and p110gamma: a prototype for new anti-inflammatory drugs. Chem. Biol. *17*, 123–134.

Winer, E.S., Ingham, R.R., and Castillo, J.J. (2012). PCI-32765: a novel Bruton's tyrosine kinase inhibitor for the treatment of lymphoid malignancies. Expert Opin. Investig. Drugs *21*, 355–361.

